Drugs in R&D (2024) 24:51–68
https://doi.org/10.1007/s40268-023-00450-6

ORIGINAL RESEARCH ARTICLE

Drug–Drug Interaction Studies of Esmethadone (REL-1017) Involving CYP3A4- and CYP2D6-Mediated Metabolism

Nicola Ferri[1,2] · Sara De Martin[3] · James Stuart[4] · Sergio Traversa[4] · Franco Folli[5] · Marco Pappagallo[4] · Cedric O'Gorman[4] · Clotilde Guidetti[6] · Andrea Mattarei[3] · Charles E. Inturrisi[4] · Paolo L. Manfredi[4]

Accepted: 2 November 2023 / Published online: 27 November 2023

Abstract

Background and Objective Esmethadone (dextromethadone; d-methadone; S-methadone (+)-methadone; REL-1017) is the opioid inactive dextro-isomer of racemic methadone. Esmethadone is a low potency N-methyl-D-aspartate (NMDA) receptor channel blocker with higher affinity for GluN2D subtypes. Esmethadone showed robust, rapid, and sustained antidepressant effects in patients with major depressive disorder (MDD) with inadequate response to ongoing serotonergic antidepressant treatment.

Methods Here we described the results of in vitro and phase 1 clinical trials aimed at investigating the esmethadone metabolism and possible drug-drug interactions.

Results Esmethadone is primarily metabolized to EDDP (2-ethylene-1,5-dimethyl-3,3-diphenylpyrrolidine) by multiple enzymes, including CYP3A4/5 and CYP2B6. In vitro studies showed that esmethadone inhibits CYP2D6 with IC_{50} of 9.6 µM and is an inducer of CYP3A4/5. The clinical relevance of the inhibition of CYP2D6 and the induction of CYP3A4 were investigated by co-administering esmethadone and dextromethorphan (a substrate for CYP2D6) or midazolam (a substrate for CYP3A4) in healthy volunteers. The administration of esmethadone at the dosage of 75 mg (which is the loading dose administered to patients in MDD clinical trials) significantly increased the exposure (AUC) of both dextromethorphan and its metabolite dextrorphan by 2.71 and 3.11-fold, respectively. Esmethadone did not modify the pharmacokinetic profile of midazolam, while it increased C_{max} and AUC of its metabolite 1′-hydroxymidazolam by 2.4- and 3.8-fold, respectively. A second study evaluated the effect of the CYP3A4 inhibitor cobicistat on the pharmacokinetics of esmethadone. Cobicistat slightly increase (+32%) the total exposure (AUC_{0-inf}) of esmethadone.

Conclusions In summary, esmethadone demonstrated a negligible effect on CYP3A4 induction and its metabolism was not meaningfully affected by strong CYP3A4 inhibitors while it increased exposure of CYP2D6-metabolized drugs.

✉ Nicola Ferri
nicola.ferri@unipd.it

1 Department of Medicine-DIMED, University of Padua, 35122 Padua, Italy

2 Veneto Institute of Molecular Medicine, Via Giuseppe Orus 2, 35129 Padua, Italy

3 Department of Pharmaceutical and Pharmacological Sciences, University of Padua, 35122 Padua, Italy

4 Relmada Therapeutics, Coral Gables, FL 33134, USA

5 Department of Health Sciences, University of Milan, 20122 Milan, Italy

6 Child and Adolescent Neuropsychiatry Unit, Department of Neuroscience, Bambino Pediatric Hospital, IRCCS, Rome, Italy

Key Points

This study identifies the enzymes, cytochromes, implicated in the metabolism of esmethadone, a new antidepressant drug.

Clinical data indicated that esmethadone may interfere with the co-administration of other drugs metabolized by cytochrome P450 2D6.

1 Introduction

Major depressive disorder is a functionally severely disabling condition characterized by depressed mood, loss of interest in activities of daily life, lack of motivation, and cognitive dysfunction. It has been estimated that approximately 70% of patients with major depressive disorder have a comorbid chronic physical condition [1]. One important consequence of multimorbidity is polypharmacy, with an increased probability of experiencing side effects caused by a drug–drug interaction (DDI).

Esmethadone, in contrast with levomethadone, has no meaningful agonist activity at opioid receptors and no meaningful risk for abuse potential [2, 3]. Esmethadone is a low potency *N*-methyl-D-aspartate (NMDA) receptor channel blocker with higher affinity for GluN2D subtypes in the presence of physiological magnesium levels [4, 5]. Results of phase I and phase II trials showed favorable safety, tolerability, and pharmacokinetic profiles [6, 7]. Additionally, esmethadone showed robust, rapid, and sustained antidepressant effects in patients with major depressive disorder with an inadequate response to serotonergic antidepressant treatment [6]. In this study, although the majority of patients were treated with serotonergic antidepressant drugs that are metabolized by cytochrome P450 (CYP) 2D6, an enzyme known to be inhibited by methadone, the addition of esmethadone did not cause any signs or symptoms of serotonergic toxicity.

The pharmacokinetic characteristics of esmethadone were examined in prior clinical studies conducted with the synthetic analgesic methadone administered as an equal mixture of the two racemic forms and also in phase I and phase II studies of esmethadone [3, 6, 7]. Methadone is a liposoluble basic drug with a pKa of 9.2. A detectable concentration of esmethadone can be measured in the blood 15–45 min after its oral administration. Time to maximum observed concentration (T_{max}) is slightly shorter for esmethadone as compared with levomethadone (2 h vs 3 h), although the median range may vary considerably between patients (from 1 h up to 5 h) [8] and is independent from the dose [9]. This shorter T_{max} of esmethadone compared with levomethadone may reflect the pharmacological effect on gastrointestinal opioid receptors, which is exerted by levomethadone and not by esmethadone [10].

The oral bioavailability of methadone was found to be around 70–80%, similar for the two enantiomers, suggesting the absence of specific stereoselective transporters involved in intestinal absorption [8, 11]. However, a marked inter-subject variability was observed (range 36–100% [8, 11–13]). One major factor responsible for the variations of methadone bioavailability could be the inter-individual difference in CYP3A4 expression [14], from 1-fold to 30-fold in the liver and from 1-fold to 11-fold in the gut [15]. Methadone undergoes a minimal amount of enterohepatic recirculation with small secondary peaks observed in the concentration–time curve [9].

There is a general consensus that methadone is metabolized almost exclusively by the liver [16]. The main biotransformation of the two methadone enantiomers is the N-demethylation resulting in the formation of inactive metabolites, which are then excreted into urine and bile. The main metabolite, EDDP, is inactive both on opioid receptors as well as on NMDA receptors. The oxidative metabolism involves the CYP system, including CYP3A4 and the stereoselective action of CYP2B6 and CYP2C19. In particular, CYP2B6 preferentially metabolized esmethadone, CYP2C19 is more effective on levomethadone, and CYP3A4 shows no preference [17]. Although the involvement of CYP3A4 in methadone clearance has been considered relevant [17–21], a clinically relevant interaction with CYP3A4 inhibitors or inducers is still debated [22–27]. On these premises, we first characterize the in vitro inhibitory potential of esmethadone on the activities of the main CYP and 5′-diphospho-glucuronosyltransferase (UGT) isoforms. We then presented clinical trials conducted to determine the in vivo effect of esmethadone on CYP3A4 and CYP2D6 activities and the influence of CYP3A4 inhibition on the disposition of esmethadone. Finally, we evaluate the absorption, metabolism, and excretion of [^{14}C]-esmethadone in an open-label single-dose study conducted in healthy male subjects.

2 Methods

2.1 Inhibitory Assay on CYP Activities in Human Liver Microsomes (HLMs)

Human liver microsomes (HLMs) from 150 individuals (79 male and 71 female) were obtained from BioIVT (Baltimore, MD, USA) and Corning (Woburn, MA, USA) and stored at approximately – 70 °C. A single CYP-selective substrate concentration was used, approximating the concentration of the substrate that gives half the maximum reaction velocity (Km) for each CYP assay. Assays were performed in the absence and presence of esmethadone (0.2–200 μM) to determine its inhibitory activity. The assays were run under linear conditions.

The Hamilton Microlab Star automated liquid handling system conducted all sample preparation steps. For direct inhibition assays, the microsomal incubation mixture containing HLMs, buffer, the marker substrate, and esmethadone (or positive/negative controls) were added to a chilled 96-well assay plate before being placed onto a heater shaker at 37 °C for a 10-min pre-incubation period.

The total organic solvent contribution in the incubation mixture was ≤ 1%. The incubation was initiated by the addition of NADPH (1 mM) and terminated by the addition of stop solution (acetonitrile containing an internal standard). After incubation, plates were centrifuged at 1000 rpm for approximately 5 min, and supernatants were transferred to a separate 96-well plate for a liquid chromatography–mass spectrometry (LC–MS) analysis. Analyte concentrations were quantitated and interpolated from standard curves of the authentic analyte. All sample and control incubations were performed in triplicate. Details of the incubation conditions for each assay are presented in Table 1.

Incubations for direct inhibition assessment were conducted at eight concentrations of the test substance (0.200, 0.537, 1.44, 3.86, 10.4, 27.8, 74.6, and 200 μM) and at a CYP-selective marker substrate concentration corresponding to its Michaelis–Menten constant (Km) value. The inhibition constant (Ki) for CYP2D6 was estimated using the same assay conditions, with the following exception: five concentrations of the marker substrate were chosen (2, 5, 10, 20, and 50 μM). Incubation mixtures including HLMs, test substance, and marker substrate in an assay buffer were pre-incubated at 37 °C for 10 min before initiation with the addition of the cofactor NADPH (1 mM), opportunely pre-warmed. Incubations were terminated by the addition of chilled acetonitrile, containing a stable-labeled internal standard specific to the CYP substrate, after the appropriate incubation time. Control incubations consisted of pre-incubation samples with esmethadone in the absence of NADPH, esmethadone solvent control, and time-dependent inhibitor and solvent control in the absence and presence of NADPH. All incubations were performed in triplicate.

The in vitro kinetic parameters Kl for time-dependent inhibition were estimated using the same assay conditions with the following exception: eight concentrations of esmethadone (0.1–25 μM), and incubation time (seven time points, 0–30 min). The extent of microsomal protein binding was investigated using an equilibrium dialysis for 5 h at 37 °C, with 1, 10, and 100 μM of esmethadone in 0.05, 0.1, and 0.5 mg/mL of HLM. Esmethadone was demonstrated to be stable under these testing conditions.

2.2 Inhibitory Assay on UGT Enzymes by Esmethadone in HLMs

Incubations were conducted in triplicate with up to eight concentrations of esmethadone (0.200, 0.537, 1.44, 3.86, 10.4, 27.8, 74.6, and 200 μM). All incubations were conducted at a probe substrate concentration corresponding to its Michaelis–Menten constant (Km value). Human liver microsomes were activated by pre-incubation on wet ice for at least 15 min with alamethicin (50 μg/mg protein). Incubation mixtures, including activated HLM, marker substrate, and assay buffer (Tris-HCl buffer [50 mM, pH 7.4] containing 150 mM of KCl and 10 mM of $MgCl_2$), with or without a test article, were pre-incubated at 37 °C for 5 min before initiation with the addition of pre-warmed uridine diphosphate glucuronic acid (5 mM). The final organic solvent contribution was ≤ 2%. Incubations were terminated by the addition of a chilled stop reagent containing an internal standard.

Table 1 CYP activity assays

CYP activity	Substrate (μM)	Protein (mg/mL)	Time (min)	Internal standard	Analyte	Positive control (μM)
CYP1A2	110	0.063	10	Phenacetin *O*-deethylase	Acetaminophen	Fluvoxamine (0.5)[a] Furafylline (3)[b]
CYP2B6	120	0.063	10	Bupropion hydroxylase	Hydroxybupropion	Orphenadrine (600)[a] ThioTEPA (20)[b]
CYP2C8	1.5	0.013	10	Amodiaquine *N*-deethylase	Desethylamodiaquine	Montelukast (0.1)[a] GEM (40)[b]
CYP2C9	6	0.1	5	Diclofenac 4′-hydroxylase	4′-Hydroxydiclofenac	Sulfaphenazole (5)[a] Tienilic acid (10)[b]
CYP2C19	50	0.063	10	*S*-Mephenytoin 4′-hydroxylase	4′-Hydroxymephenytoin	Nootkatone (20)[a] Esomeprazole (8)[b]
CYP2D6	10	0.063	10	Dextromethorphan *O*-demethylase	Dextrorphan	Quinidine (0.3)[a] Paroxetine (2)[b]
CYP3A4/5	65	0.1	5	Testosterone 6β-hydroxylase	6β-Hydroxytestosterone	Ketoconazole (0.2)[a] Erythromycin (100)[b]
CYP3A4/5	1.5	0.063	5	Midazolam 1′-hydroxylase	1′-Hydroxymidazolam	Ketoconazole (0.2) Troleandomycin (10)[b]

CYP cytochrome P450, *min* minutes

[a]Positive control for direct inhibition

[b]Positive control for time-dependent inhibition (pre-dilution concentration)

Samples were centrifuged for 5 min, and supernatant was transferred to clean vials and stored at 2–8 °C prior to analysis by LC-MS. Control incubations included a test article solvent control (no test article), positive control inhibitor, and an additional solvent control (as needed) specific to the positive control inhibitor. Details of the incubation conditions for each assay are presented in Table 2.

2.3 Inhibitory Assay of UGT2B15 by Esmethadone in Supersomes™

Supersomes™ expressing human recombinant UGT2B15 enzyme were obtained from Corning Discovery Labware, Inc. (Woburn, MA, USA). Supersomes™ were stored at approximately – 70 °C. Incubations were conducted in triplicate with up to eight concentrations of esmethadone (from 0.2 to 200 µM). Incubations were conducted in triplicate with up to eight concentrations of esmethadone (0.200, 0.537, 1.44, 3.86, 10.4, 27.8, 74.6, and 200 µM). All incubations were conducted at a probe substrate concentration corresponding to its Km value. Incubation mixtures, including supersomes, marker substrate, and assay buffer, with or without esmethadone, were pre-incubated at 37 °C for 5 min before initiation with the addition of pre-warmed uridine diphosphate glucuronic acid (5 mM). The final organic solvent contribution was ≤ 1%. Incubations were terminated by the addition of chilled methanol containing an internal standard. Samples were centrifuged for 5 min, and supernatant was transferred to clean vials and stored at 2–8 °C prior to analysis by LC-MS. Control incubations included a test article solvent control (no test article), positive control inhibitor, and an additional solvent control specific to the positive control inhibitor. Details of the incubation conditions are presented in Table 3.

2.4 Evaluation of CYP450 Induction

The study was designed to assess the induction potential of esmethadone on the mRNA gene expression of CYP1A2, CYP2B6, CYP2C8, CYP2C9, CYP2C19, and CYP3A4/5. Cryopreserved human hepatocytes from a single donor were incubated for 72 ± 2 h in the presence of esmethadone and an appropriate solvent control to analyze test article cytotoxicity. Following treatment, cytotoxicity was evaluated using the CellTiter 96 AQ_{ueous} Assay Kit (MTS assay; Promega, Madison, WI, USA). Cryopreserved hepatocytes from three human donors were separately incubated with esmethadone, a prototypical inducer for each enzyme, a non-inducer, and an appropriate solvent control for esmethadone, a non-inducer, or each prototypical inducer, as applicable

Table 2 UGT activity assays

Assay (UGT activity)	Substrate (µM)	Protein (mg/mL)	Time (min)	Analyte	Internal standard	Positive control (µM)
UGT1A1	20	0.2	20	β-Estradiol 3-β-D-glucuronide	Niflumic acid	Tangeritin (60)
UGT1A3	35	0.2	20	Chenodeoxycholic acid 24-Acly-β-D-glucuronide	Tolbutamide	Lithocholic acid (100)
UGT 1A4	50	0.2	10	Trifluoperazine-*N*-β-D-glucuronide	Tolbutamide	Hecogenin (20)
UGT1A6	7500	0.2	10	Serotonin glucuronide	Serotonin-d4 glucuronide	Ketoconazole (100)
UGT1A9	60	0.2	20	Propofol β-D-glucuronide	d17-Propfol glucuronide	Diflunisal (60)
UGT2B7	2000	0.2	10	3′-Azido-3′-deoxythymidine β-D-glucuronide	3′-Azido-3′-deoxythymidine-d3 β-D-glucuronide	Mefenamic acid (30)

min minutes

Table 3 UGT2B15 activity assay

Assay (UGT activity)	Substrate (µM)	Protein (mg/mL)	Time (min)	Analyte	Internal standard	Positive control (µM)
UGT2B15	20	0.05	10	7-Hydroxy-4-(trifluoro-methyl) coumarin glucuronidation	4-Methylumbelliferyl-B-D-glucuronide	Ketoconazole (25)

min minutes

for 72 ± 2 h to analyze mRNA expression. Gene expression was evaluated using the comparative cycle time methodology using the CYP enzyme-specific gene probes. All sample incubations were performed in triplicate.

2.5 Cell Culture

Thawing medium (Universal Cryo Recovery Medium) for hepatocytes was purchased from In Vitro ADMET Laboratories (iVAL, Columbia, MD, USA). Hepatocyte culture medium (Williams' E Medium [WEM]), supplements (Hepatocyte Plating Supplement Pack and Hepatocyte Maintenance Supplement Pack), and GelTrex Matrix (LDEV-free, Reduced Growth Factor) were purchased from Gibco (Thermo Fisher Scientific, Waltham, MA, USA). The supplements were added to the WE prior to use as plating medium (sWEP) or as culture maintenance medium (warmed supplemented WEM). All media were stored at 5 °C.

2.6 Esmethadone Solution Preparation

The hepatocyte cultures were dosed with 100-µL aliquots of warmed supplemented WEM with esmethadone stock solutions in methanol to achieve final concentrations of 0.3, 3, 10, 30, and 50 µM (initial cytotoxicity), 0.3, 1, 2.5, 5, 10, 25, and 50 µM (gene expression), and 1, 10, and 50 µM (enzyme activity). The methanol final concentration was 1% (v/v). A solvent control solution, consisting of warmed supplemented WEM containing methanol at 1% (v/v), was also prepared. Stock and tested solutions were prepared fresh on each day an assay was performed. The concentrations in test article solutions were based on recorded weights and volumes.

2.7 Positive Control Inducers

Solutions of a non-inducer and prototypical inducers of CYP1A2, CYP2B6, CYP2C8, CYP2C9, CYP2C19, and CYP3A4/5 were prepared in warmed supplemented WEM immediately prior to each dose. The identity, final concentration, and vehicle composition of each solution are detailed in Table 4.

2.8 Application of Esmethadone, Prototypical Inducer, and Non-Inducer

Following acclimation of the hepatocyte cultures overnight, the culture medium was removed from the wells and replaced with the appropriate test article, prototypical inducer, non-inducer, or solvent control dosing solution (0.1 mL/well). This dosing was repeated approximately every 24 h, as applicable, such that the hepatocytes were exposed for a total of 72 ± 2 h. Prior to induction experiments, hepatocyte cultures from one donor were dosed with test article (0.3, 3, 10, 30, and 50 µM) and solvent control for 72 ± 2 h.

2.9 Determination of Gene Expression for CYP450 Enzymes

Test and control solutions were removed from hepatocyte cultures after 72 ± 2 h of exposure. Hepatocytes were washed with Dulbecco's phosphate-buffered saline, subsequently lysed, and harvested using the mRNA Catcher Plus kit (Invitrogen, Carlsbad, CA, USA). The mRNA was transcribed to cDNA on the same day of extraction using TaqMan Reverse Transcription reagents (Applied Biosystems, Foster City, CA, USA). Remaining mRNA was stored at – 70 °C, and cDNA was stored at – 20 °C until further analysis. Relative concentrations of CYP1A2, CYP2B6, CYP2C8, CYP2C9, CYP2C19, and CYP3A4 mRNA were determined by real-time polymerase chain reaction using QuantStudio 6 Flex (Applied Biosystems), TaqMan Fast Advanced Master Mix (Applied Biosystems), and enzyme-specific probes (Applied Biosystems). Each CYP450 mRNA was normalized to the mRNA of the endogenous control (GAPDH) in each sample. For each CYP gene that is induced by the test article, the maximum increase in gene expression (E_{max}) and the concentration of test article

Table 4 Cytochrome P450 inducing assays

CYP enzyme induced	Prototypical inducer/non-inducer	Vehicle	Concentration (µM)
CYP1A2	Omeprazole	0.1% DMSO in sWEM	50
CYP2B6	Phenobarbital	0.1% DMSO in sWEM	1000
CYP2C8, CYP2C9, CYP2C19	Rifampicin	0.1% DMSO in sWEM	20
CYP3A4/5	Rifampicin	0.1% DMSO in sWEM	10
Non-inducer	Flumazenil	0.1% DMSO in sWEM	20

A solution of 0.1% dimethyl sulfoxide (DMSO) in supplemented Williams' E Medium (sWEM) was prepared for use as a solvent control. DMSO percentages are volume/volume (v/v)

CYP cytochrome P450, *DMSO* dimethyl sulfoxide, *sWEM* supplemented Williams' E Medium

resulting in a half-maximum increase (EC_{50}) were calculated, as applicable.

2.9.1 Uptake Transporter Assay

Transfected HEK293 cells were seeded into 24-well poly-D-lysine-treated plates at an appropriate density and were incubated for 3–4 h at 37 °C in an atmosphere of 5% CO_2 and saturated humidity. The media was then replaced with fresh sDMEM and the cells were maintained at 37 °C in an atmosphere of 5% CO_2 and saturated humidity until used for an assay, approximately 24 h after plating. OATP1B1 and OATP1B3 cells and associated vector control were treated with 5 mM of sodium butyrate and multidrug and toxin extrusion pump 1 (MATE1) and MATE2-K and associated vector controls were treated with 2 mM of sodium butyrate the day prior to the assay.

Incubations to determine uptake were performed according to the following procedure. After removal of the culture medium by aspiration, each well was washed once with transport buffer and then pre-incubated with transport buffer for 15 (MATEs only) or 30 min, followed by aspiration of buffer. For MATE1 and MATE2-K, cells were pre-treated with 40 mM of NH4Cl in transport buffer for 20 min at 37 °C, followed by aspiration of buffer. The uptake was initiated by adding 300 µL of pre-warmed (37 °C) working solution to each well. The incubation time for uptake of probe substrates was 2 (MATEs only) or 5 min. Incubations were conducted at 37 °C and terminated by quickly aspirating the working solution and rinsing the cells two or three times with 400 µL of a solution of ice-cold transport buffer. The cells were then lysed by three freeze-thaw cycles in transport buffer. The cell lysate from appropriate wells was analyzed by liquid scintillation counting (LSC) to determine the amount of radioactivity of probe substrates. The concentrations of the test article in the cell lysate samples and test solutions were determined using LC–MS. Samples were stored at – 20 °C until analysis, as applicable. Parallel cell cultures were prepared for the determination of protein amounts per well on each day of experimentation. Cells were lysed in HBSS containing 0.1% (v/v) Triton X-100 and samples were stored at – 70 °C until the protein analysis.

Uptake of esmethadone (0.3, 3, and 30 µM) by each transporter in the presence of a vehicle or selective inhibitor, and by the vector control, was conducted according to the uptake incubation procedure for 2 min (MATE only) or 5 min. Uptake of a probe substrate by each transporter in the presence of a vehicle or selective inhibitor and by the vector control was performed as controls. Probe substrate information for the corresponding transporters is summarized in Table 5.

2.9.2 Efflux Transporter Assay

Caco-2 cells were plated in 24-well Costar Transwell® polyester membrane inserts (pore size 0.4 µm) in sDMEM containing 10% (v/v) fetal bovine serum, 2 mM of glutamine, 1% (w/v) non-essential amino acids, 100 units/mL of penicillin, and 100 µg/mL of streptomycin. Cells suspended in sDMEM were seeded onto wet and equilibrated membranes at an initial density of 2×10^5 cells/mL. The monolayers were maintained at 37 °C in an atmosphere of 5% CO_2 with saturated humidity for 24 days in order for monolayers to form and achieve full expression of membrane proteins. During this culture period, the medium was replaced at least three times each week.

Apparent permeability was determined in both the apical to basolateral and basolateral to apical directions. Measurement of the trans-epithelial electrical resistance with a World Precision Instruments (WPI), Inc. volt-ohm meter prior to and following experimentation was used to confirm the formation of tight junctions in the monolayers. After aspiration of the culture medium, the Transwell inserts were pre-incubated with a Caco-2 transport buffer-containing vehicle for 30 min in the upper and lower compartments. A fresh transport buffer-containing vehicle or inhibitor, as appropriate, was added to the receiver compartments, and a test article working solution with

Table 5 Uptake transporter control, substrates, and inhibitors

Transporter	Probe substrate (µM)	Selective inhibitor (µM)
OAT1	^{14}C-para-aminohippurate (1)	Probenecid (200)
OAT3	^{3}H-estrone-3-sulfate (1)	Probenecid (200)
OCT1	^{14}C-tetraethylammonium (5)	Quinidine (256)
OCT2	^{14}C-metformin (1)	Quinidine (256)
OATP1B1	^{3}H-estradiol-17β-D-glucuronide (0.5)	Cyclosporine A (10)
OATP1B3	^{3}H-cholecystokinin octapeptide (1)	Cyclosporine A (10)
OATP2B1	^{3}H-estrone-3-sulfate (1)	Rifamycin SV (30)
MATE1	^{14}C-tetraethylammonium (5)	Cimetidine (100)
MATE2-K	^{14}C-tetraethylammonium (5)	Cimetidine (100)

MATE multidrug and toxin extrusion

or without inhibitors was added to the corresponding donor compartments to initiate the transport.

The incubation was conducted at 37 °C for 2 h and terminated by collection of the donor and receiver samples. The control samples and working solutions were analyzed by LSC to determine the amount of radioactivity of the probe. The concentrations of the test article in the samples and test article working solutions were determined using LC–MS, as applicable. Samples were stored at − 20 °C until analysis, as appropriate.

To confirm that the monolayers were suitable, the apparent permeabilities of paracellular (mannitol) and transcellular (caffeine) marker compounds and of probe substrates were determined. Cell monolayers were incubated with ^{14}C-mannitol (10 µM), ^{14}C-caffeine (5 µM), ^{3}H-digoxin (1 µM), and ^{3}H-estrone-3-sulfate (0.1 µM) for 2 h according to the efflux incubation procedure on each day of experimentation.

For each transporter, the apparent permeability of esmethadone (0.3, 3, 30, and 50 µM) was assessed in the presence of a vehicle or selective inhibitor according to the efflux incubation procedure. Negative inhibitors were included in parallel to confirm the specificity of interaction. The permeability of each probe substrate was assessed in the presence of a vehicle or known inhibitor as a control. Probe substrate and known inhibitor information is summarized in Table 6.

2.9.3 Data Analysis

Statistics were limited to descriptive statistics, such as means, standard deviations, relative standard deviations, and linear regression analyses, where appropriate. Activity and half-maximal inhibitory concentration (IC_{50}) calculations, as applicable, as well as additional kinetic calculations, were determined using SoftMax Pro, SigmaPlot Version 12.5, or Microsoft Excel Version 16.0. Outliers among replicates were identified in accordance with Covance SOPs.

2.10 Clinical Studies

2.10.1 Study 1 (hADME)

This was an open-label study of the absorption, distribution, metabolism, and excretion of [^{14}C]-esmethadone following a single oral dose in healthy male subjects. Metabolite profiles and identification of [^{14}C]-esmethadone-related radioactivity were determined in plasma, urine, and feces samples collected from healthy male subjects after a single 25-mg (150-µCi) oral dose of [^{14}C]-esmethadone in the fasted state. Plasma samples were collected 0.5, 1, 1.5, 2, 3, 6, 8, 12, and 24 h post-dose. Urine samples were collected at 0–4, 4–8, 8–12, 12–24, 24–48, 48–72, 72–96, 96–120, 120–144, 144–168, and 168–192 h post-dose. Fecal samples were collected at 0–24, 24–48, 48–72, 72–96, 96–120, 120–144, 144–168, 168–192, 192–216, and 216–240 h post-dose. Plasma samples were pooled by individual at maximum observed concentration (C_{max}) and across timepoints to generate a 0.5- to 24-h area under the concentration–time curve (AUC) representative of pooled samples. Urine and fecal homogenate samples were pooled across collection intervals by subject to generate individual urine and fecal homogenate pools. Plasma, urine, and feces samples were stored at approximately – 70 °C before and after analysis. Subjects were discharged on day 15 if one of the following conditions occurred: plasma radioactivity levels were below the limit of quantitation for two consecutive collections, if ≥ 90% mass balance was recovered, and if ≤ 1% of total radioactive dose was recovered in the combined excreta (urine and feces) in two consecutive 24-h periods.

No formal statistical assessment of sample size was conducted. The sample size chosen of eight male subjects for this study is commonly adopted in human radiolabeled studies and was considered sufficient to achieve the objectives of the study. Up to eight subjects were enrolled to ensure that six subjects complete the study.

2.10.2 Biochemical Analysis

Plasma samples were pooled by individual to generate a 0.5- to 24-h AUC representative. For each subject, a C_{max} was also analyzed. The radioactivity in each pooled sample was determined by LSC. Two 2-g aliquots of each AUC-pooled plasma sample were combined with 6 mL of acetonitrile. Each mixture was sonicated, vortex mixed, and centrifuged, and the supernatant was removed. The extraction was repeated, and the respective supernatants were combined. Duplicate aliquots were analyzed by LSC to determine extraction recoveries, which ranged from 78.3 to 94.9%.

Urine and fecal samples were pooled in proportion to the weight of urine and feces collected in each sampling period. The radioactivity in each pooled sample was determined by LSC.

Approximately 2.3–2.6 g of each pooled feces sample was combined with 6 mL of acetonitrile. Each mixture was

Table 6 Efflux transporter substrates and inhibitors (using Caco-2 cells)

Transporter	Probe substrate (µM)	Selective inhibitor (µM)	Negative inhibitor (µM)
P-gp	^{3}H-digoxin (1)	Zosuquidar (2)	Ko143 (1)
BCRP	^{3}H-estrone-3-sulfate (0.1)	Ko143 (1)	Zosuquidar (2)

BCRP breast cancer resistant protein, *P-gp* P-glycoprotein

sonicated, vortex mixed, and centrifuged, and the supernatant was removed. The extraction was repeated, and the respective supernatants were combined. Duplicate aliquots were analyzed by LSC to determine extraction recoveries, which ranged from 85.1 to 111%.

2.10.3 Metabolite Profiling and Identification

All processed plasma, urine, and fecal homogenate samples were analyzed by liquid chromatography-high resolution mass spectrometry, with eluent fractions collected at 10-s intervals into 96-well plates containing solid scintillant. Radioactivity in each well was determined using a MicroBeta2 analysis, and radiochemical profiles were generated based on radioactivity counts. Quantitation of the metabolites present in the plasma, urine, and feces was based on the profiles of radioactivity.

2.10.4 Study 2 (DDI Perpetrator)

This was an open-label, fixed-sequence, single-dose, and multiple-dose DDI study as illustrated in Fig. 1. Eligible participants received a single oral dose of midazolam 2 mg on day 1 and a single oral dose of dextromethorphan 30 mg on day 2. After a washout period of 48 h on day 4, participants received a single (75-mg loading oral dose) of esmethadone in combination with a single oral dose of dextromethorphan 30 mg. From days 6–18, esmethadone was administered at an oral dose of 25 mg once daily and, on day 19, esmethadone at 25 mg was co-administered with a single oral dose of midazolam 2 mg. The pharmacokinetics of midazolam and 1′-hydroxymidazolam was characterized over 24 h on day 1 and day 19, the pharmacokinetics of dextromethorphan and dextrorphan was characterized over 48 h on day 2 and on day 4. The pharmacokinetics of esmethadone was characterized over 48 h on day 4 and over 24 h starting on day 19 (Fig. 1). Pharmacokinetic blood samples were collected for midazolam and its metabolite (1′-hydroxymidazolam) on day 1 and day 19 before dosing and 0.167 (10 min), 0.333 (20 min), 0.5, 0.75, 1, 1.5, 2, 3, 4, 5, 6, 8, 12, 16, and 24 h post-dose. Pharmacokinetics blood samples were collected for dextromethorphan and its metabolite (dextrorphan) on day 2 and day 4 before dosing and 0.5, 1, 2, 2.5, 3, 3.5, 4, 6, 8, 12, 16, 24, and 48 h post-dose. Pharmacokinetics of blood samples were collected for esmethadone on day 4 before dosing and 0.5, 1, 1.5, 2, 2.5, 3, 4, 6, 8, 12, 24, and 48 h post-dose. Pharmacokinetics blood samples were collected − 10 min prior to dosing on days 13, 17, and 18 for esmethadone and on day 19 before dosing and 0.5, 1, 1.5, 2, 2.5, 3, 4, 6, 8, 12, and 24 h post-dose.

Twenty-eight (28) male or non-childbearing potential female individuals were planned to be enrolled for participation in this study. The study was powered for the AUC and C_{max} comparison of midazolam and should have been sufficient to demonstrate no DDI. Based on data from previous studies, the intraparticipant coefficients of variation for midazolam should have been approximately 22% for AUC and C_{max}. Thus, with this expected coefficient of variation and assuming a ratio of AUC and C_{max} within 0.95 and 1.05, the study should have had a power of at least 80% to show no DDI, i.e., 90% confidence intervals of test: reference within 80–125% for AUC from time zero extrapolated to infinity (AUC_{0-inf}), AUC from time zero to the time of the last quantifiable concentration (AUC_{0-t}), and C_{max} with 24 participants. To account for possible study dropouts, up to 28 participants were included in the study. This sample size was also appropriate to investigate the inhibitory effect of esmethadone on the pharmacokinetics of dextromethorphan.

2.10.5 Study 3 (DDI Victim)

This was an open-label single-center DDI study to assess the effect of cobicistat on the pharmacokinetic profile of esmethadone in healthy adult participants as illustrated in Fig. 2. On day 1, participants received a single oral dose of esmethadone 25 mg. On days 11–20, participants received an oral dose of cobicistat 150 mg once daily. On day 15, participants received a single dose of esmethadone 25 mg in combination with a single dose of cobicistat 150 mg. Prior to each dosing day, participants were required to fast overnight for ≥ 10 h. The participants fasted for 4 h post-dose. All doses were administered 30 min after consuming a snack or light meal. Pharmacokinetic samples for esmethadone were collected at the following times on day 1: pre-dose (0 h), 0.5,

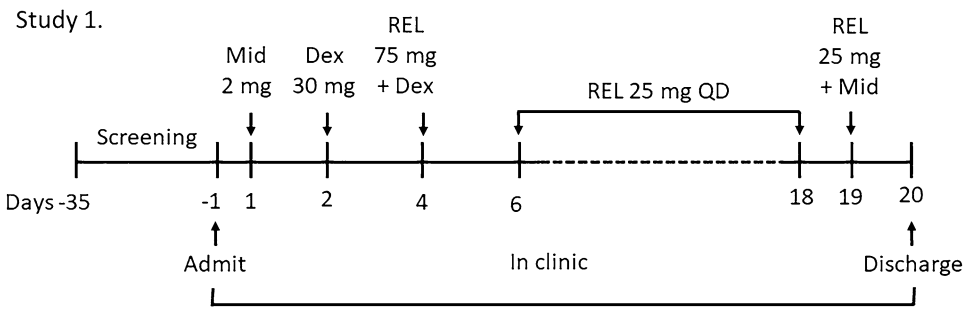

Fig. 1 Schematic overview of study 2. *Dex* dextromethorphan, *Mid* midazolam, *QD* once daily, *REL* esmethadone

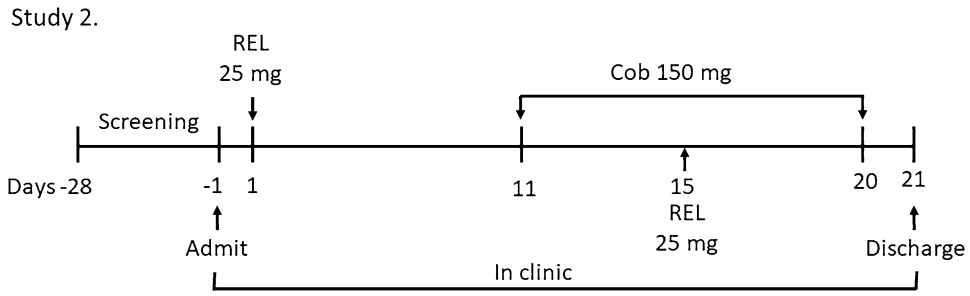

Fig. 2 Schematic overview of study 3. *Cob* cobicistat, *REL* esmethadone

1, 1.5, 2, 2.5, 3, 4, 6, 8, 12, 24, 48, 72, 96, 120, and 144 h post-dose and at the following times on day 15: pre-dose (0 h), 0.5, 1, 1.5, 2, 2.5, 3, 4, 6, 8, 12, 24, 48, 72, 96, 120, and 144 h post-dose. The pre-dose pharmacokinetic sample on day 15 may was used for the pre-dose trough sample.

Twenty-eight (28) participants were enrolled in this study (approximately 50% for each sex) to ensure 24 completers. A sample size of 24 participants was considered adequate to assess the pharmacokinetic parameters of esmethadone when administered alone and in combination with cobicistat.

2.10.6 Subjects

Subjects were male or non-childbearing potential female individuals (for studies 2 and 3) of any race between 18 and 65 (55 for studies 2 and 3) years of age, body mass index between 18.0 and 35.0 kg/m^2, in good health, determined by no clinically significant findings from medical history and vital sign measurements, and clinical laboratory evaluations, a 12-lead electrocardiogram at screening, and a negative physical examination. A complete physical examination included assessments of the head, eyes, ears, nose, throat, neck, chest, lungs, abdomen, musculoskeletal, dermatological, cardiovascular/peripheral vascular, and general neurological. Demographic characteristics of the subjects enrolled in these studies are listed in Tables S1 and S3 of the Electronic Supplementary Material (ESM).

We excluded CYP2B6 poor metabolizers, as determined by genotyping during screening, and subjects with a significant history or clinical manifestation of any metabolic, allergic, dermatological, hepatic, renal, hematological, pulmonary, cardiovascular, gastrointestinal, neurological, respiratory, endocrine, or psychiatric disorder. Additional exclusion criteria were history of significant hypersensitivity, intolerance, or allergy to any drug compound, food, or other substance, disorders or history of any condition that may interfere with drug absorption, distribution, metabolism, or excretion, or a history of malabsorption or previous gastrointestinal surgery that could affect drug absorption or metabolism. A clinically significant abnormal electrocardiogram at screening, including a QT interval corrected for heart rate using Fridericia's formula > 450 ms or a family history of long QT syndrome were additional exclusion criteria. A detailed description of inclusion and exclusion criteria can be found in the supporting information.

2.10.7 Bioanalytical and Pharmacokinetic Analysis (Studies 2 and 3)

Blood samples were obtained to determine the pharmacokinetic profile and exposure of esmethadone after each treatment. The following pharmacokinetic parameters were calculated for midazolam, 1′-hydroxymidazolam, dextromethorphan, dextrorphan, and esmethadone in plasma: (1) C_{max}, T_{max}; (2) last quantifiable concentration; (3) time of the last quantifiable concentration; (4) elimination rate constant; (5) terminal half-life; (6) AUC_{0-t}; (7) AUC_{0-inf}; (8) the percentage of AUC_{0-inf} based on extrapolation, apparent clearance (for midazolam and dextromethorphan only); and (9) apparent volume of distribution (midazolam and dextromethorphan only). The pharmacokinetic analysis was performed using noncompartmental methods in Phoenix® WinNonlin® (Version 8.1; Certara, L.P) in conjunction with the Internet-accessible implementation of Pharsight® Knowledgebase Server™ (PKSO; Version 4.0.4; Certara, L.P.).

2.11 Statistical Analysis

2.11.1 Study 2

The effect of esmethadone on the pharmacokinetics of victim probe substrates (midazolam and dextromethorphan) was evaluated using GLM procedures in SAS®. An analysis of variance (ANOVA) was performed on the ln-transformed C_{max}, AUC_{0-t}, and AUC_{0-inf} of midazolam, 1′-hydroxymidazolam, dextromethorphan, and dextrorphan. The ratio of geometric means (day 4/day 2 for dextromethorphan and day 19/day 1 for midazolam) and 90% confidence intervals for the ratio of geometric means, based on least-squares means from the ANOVA of the ln-transformed data, were calculated for C_{max}, AUC_{0-t}, and AUC_{0-inf}. An ANOVA was also performed on untransformed elimination half-life. The magnitude of any potential differences in victim

probe substrate exposure in the presence of esmethadone was described using the US Food and Drug Administration (FDA) guidance for clinical drug interaction studies (2020) [28]. A non-parametric analysis (Wilcoxon's signed-ranked test) was performed on T_{max}.

2.11.2 Study 3

The DDI of esmethadone and cobicistat was evaluated using an ANOVA on log-transformed pharmacokinetic parameters: AUC_{0-t}, AUC_{0-inf}, and C_{max} (esmethadone + cobicistat/esmethadone alone). Conclusions regarding the DDI was based on the ratio of the geometric means (test/reference) for AUC_{0-t}, AUC_{0-inf}, and C_{max} and the 90% confidence interval for this ratio. No interaction was concluded if the 90% confidence intervals were fully contained within the limits of 80.0% and 125.0%. If test/reference ratios for AUCs were 500% or more, esmethadone was categorized as a sensitive CYP3A4 substrate, if test/reference ratios for AUCs were 200–499%, esmethadone was categorized as a moderately sensitive CYP3A4 substrate, and if test/reference ratios for AUCs were 125–199%, esmethadone was categorized as a mildly sensitive CYP3A4 substrate. Statistical analyses were performed using SAS®.

3 Results

3.1 In Vitro Studies

Esmethadone was first evaluated for its in vitro inhibitory activities on several human liver CYP and human UGT enzymes. As summarized in Table 7, esmethadone showed some inhibitory activity on different CYP enzymes, including 2C19, 2D6, and 3A4/5 as well as on UGT2B15. However, the IC_{50} values for CYP2C19, CYP3A4/5, and UGT2B15 were too high to be considered clinically relevant. The only exception is represented by CYP2D6, where the IC_{50} value (9.6 µM) was not far from the maximal exposure of esmethadone (C_{max}) observed in a phase I clinical trial, which in one subject reached 3.2 µM [7].

The microsomal protein binding was low overall and exhibited protein and test article concentration dependence, with decreasing binding corresponding to increased esmethadone concentrations (possibly due to saturation of binding) but increasing binding with increased HLM content (Table 8). Based on the esmethadone fraction unbound, corrected unbound IC_{50} values were generated. The unbound IC_{50} value for CYP2D6 was 8.28 µM and the unbound K_i ($K_{i,u}$) was 1.74 µM (Table 7).

Further experiments to determine the inhibition constant K_i and the type of inhibition were conducted for CYP2D6. The results for CYP2D6 (dextromethorphan O-demethylase) inhibition by esmethadone are shown in Fig. S1 of the ESM. The K_i was determined to be 2.02 µM for CYP2D6 with mixed (competitive and non-competitive) inhibition.

In vitro studies with recombinant CYP isoforms demonstrated that esmethadone is primarily metabolized to EDDP by multiple enzymes, including CYP2B6, CYP2C8, CYP2C19, CYP2D6, and CYP3A4/5 (Fig. 3). EDDP

Table 8 Summary of microsomal protein binding by esmethadone

HLM concentration	Percent unbound esmethadone		
(mg/mL)	1 µM	10 µM	100 µM
0.05	91.5	95.2	99.4
0.1	57.7	74.3	93.2
0.5	55.8	62.1	65.5

HLM human liver microsome

Table 7 Inhibitory activity of esmethadone on human liver CYP and UGT enzymes

Enzyme	Conclusion	IC_{50} (µM)	$IC_{50,u}$ (µM)	Enzyme	Conclusion	IC_{50} (µM)
CYP1A2	No	NA	NA			
CYP2A6	Yes	> 200	NA	UGT1A1	Yes	> 200
CYP2B6	Yes	> 200	NA	UGT1A3	Yes	> 200
CYP2C8	Yes	> 200	NA	UGT1A4	Yes	> 200
CYP2C9	Yes	> 200	NA	UGT1A6	No	NA
CYP2C19	Yes	174	150	UGT1A9	Yes	> 200
CYP2D6	Yes	9.63 K_i = 2.02	8.28 $K_{i,u}$ = 1.74	UGT2B7	Yes	> 200
CYP3A4/5[a]	Yes	123	103	UGT2B15	Yes	139
CYP3A4/5[b]	Yes	66.2	56.9			

CYP cytochrome P450, IC_{50} concentration of esmethadone that inhibits 50% of the enzyme activity, $IC_{50,u}$ IC_{50} unbound, *Ki* inhibition constant, *NA* not applicable

[a]Testosterone 6β-hydroxylase

[b]Midazolam 1′-hydroxylase

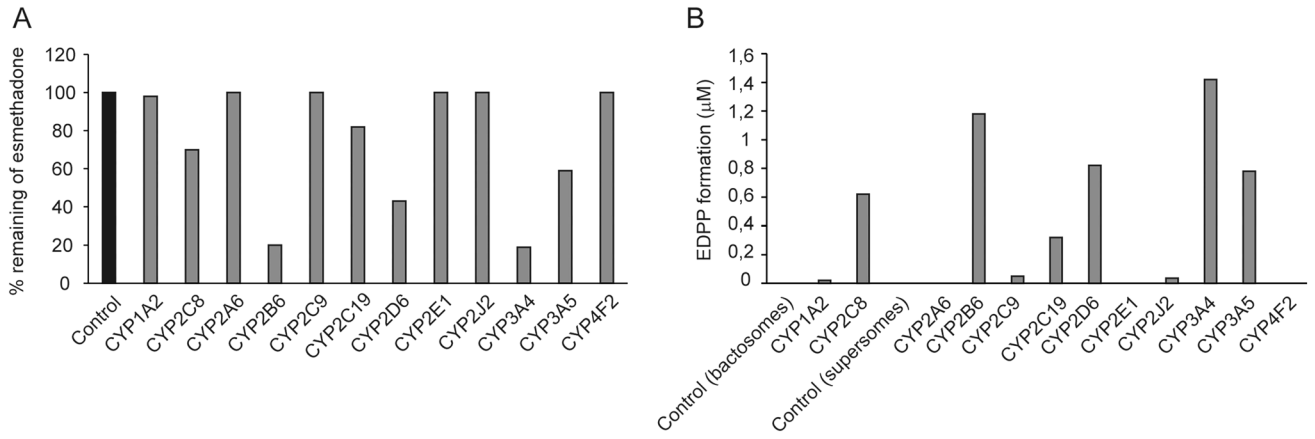

Fig. 3 In vitro metabolism of esmethadone. **A** Esmethadone was incubated with recombinant cytochrome P450 (CYP) isoforms and its metabolism was determined by LC–MS. **B** EDDP (2-ethylene-1,5-dimethyl-3,3-diphenylpyrrolidine) formation by recombinant CYP isoforms

accounted for > 85% of in vitro metabolites (data not shown). Additionally, esmethadone was demonstrated to be an inducer of CYP1A2, CYP2B6, CYP2C8, CYP2C9, and especially CYP3A4/5. Indeed, esmethadone increased by 21.4 ± 1.1-fold and 5.2 ± 4.8-fold the mRNA and enzyme activity of CYP3A4, respectively (Table 9). The effect on CYP3A4 mRNA induction was observed at EC_{50} values of 9.6 ± 3.4 μM, thus supporting a potential in vivo relevant effect (Table 9). Finally, esmethadone is not a transporter substrate, but does inhibit OCT1 (IC_{50} = 1.671 μM) and possibly P-glycoprotein (P-gp) [IC_{50} = 9.276 μM].

Table 9 CYP induction by esmethadone

Donor	mRNA levels		Enzyme activity
	Fold induction	EC_{50} (μM)	Fold induction
	CYP1A2		
1	3.61	25.7	1.09
2	4.00	3.75	1.07
3	2.24	26.3	5.01
	CYP2B6		
1	13.1	4.30	1.19
2	35.9	5.36	1.43
3	6.11	4.12	2.76
	CYP2C8		
1	5.60	2.85	1.32
2	2.70	6.42	1.10
3	2.72	5.27	2.58
	CYP2C9		
1	3.15	1.05	0.96
2	1.55	6.31	0.82
3	3.18	18.1	3.09
	CYP2C19		
1	0.98	NA	0.80
2	1.46	6.68	0.71
3	1.35	NA	1.48
	CYP3A4		
1	20.2	13.3	2.28
2	21.8	6.50	2.66
3	22.2	9.01	10.8

CYP cytochrome P450, *EC_{50}* half maximal effective concentration, *NA* not applicable

3.2 In Vivo Studies

3.2.1 Study 1

Esmethadone absorption, metabolism, distribution, and excretion were investigated in healthy volunteers at a single site using radio-labeled esmethadone. Metabolite profiles and metabolite identification of [^{14}C]-esmethadone-related radioactivity were determined in plasma, urine, and feces samples collected after a single 25-mg (150-μCi) oral dose of [^{14}C]-esmethadone. Esmethadone underwent extensive metabolism in humans after an oral dose, which was mediated predominantly by oxidative N-demethylation and, to a minimal extent, by oxidation (Fig. 4). Secondary cyclization with concomitant dehydration was extensive, while secondary glucuronidation, epoxidation, and hydrolysis were trace biotransformation pathways. Oxidative N-demethylation of esmethadone with secondary cyclization and dehydration yielded EDDP as a minor circulating metabolite and the predominant metabolite in urine and feces. Esmethadone was the most abundant circulating component in plasma, with a mean exposure ($AUC_{0.5–24}$) of 1200 ng equivalents hours [^{14}C]-esmethadone/g (ng eq. h/g) or 70.4% of the total plasma radioactivity exposure through 24 h post-dose. EDDP and oxy-esmethadone glucuronide were traced to

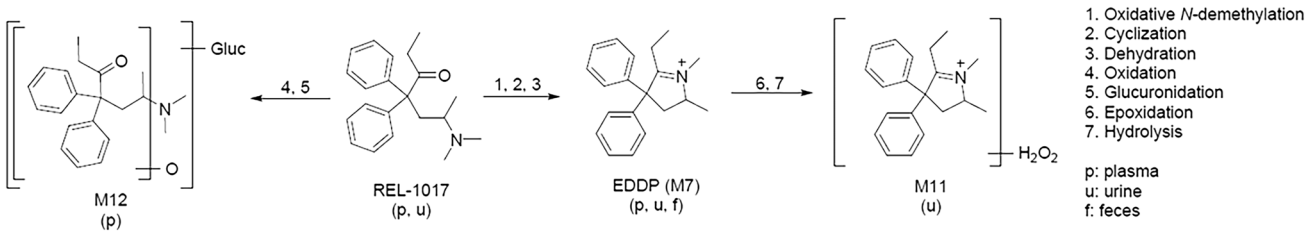

Fig. 4 Proposed biotransformation pathways of esmethadone in male human subjects. *EDDP* 2-ethylene-1,5-dimethyl-3,3-diphenylpyrrolidine, *REL* esmethadone

minor metabolites that accounted for 2.70% and 0.473% and of the total plasma radioactivity exposure, respectively.

[^{14}C]-Esmethadone-derived radioactivity was excreted in urine (53.9% of the dose) and feces (39.1% of the dose). Urinary excretion of esmethadone accounted for a mean of 13% of the dose across subjects; no fecal excretion of esmethadone was noted. EDDP was a major and the most abundant metabolite in urine and feces, accounting for 36.5% and 33.5% of the dose, respectively. The representative radiochromatogram and reconstructed ion chromatogram from analysis of a 0- to 24-h AUC-pooled plasma sample and from a 0- to 144-h pooled urine sample, after a single oral dose of 25 mg of [^{14}C]-esmethadone are shown in Fig. S2 of the ESM. Overall, these data indicate that metabolic clearance and, to a lesser extent, urinary excretion were the main routes of elimination of esmethadone in human subjects after an oral dose.

3.2.2 Study 2

The in vitro data indicated that esmethadone is metabolized by CYP3A4 and may have a potential inducing property on CYP3A4 and an inhibitory action on CYP2D6. To further investigate these possibilities, we conducted a single-center open-label DDI study. The objective was to assess the effect of esmethadone on CYP2D6 activity, the pharmacokinetic profiles of dextromethorphan (a probe substrate for CYP2D6) and its metabolite dextrorphan were studied when administered either alone or in combination with a single 75-mg loading dose of esmethadone (Fig. 1). In contrast, the possible induction on CYP3A4 was tested by administering esmethadone in combination with midazolam (probe for CYP3A4) and the pharmacokinetic profile of midazolam and its metabolite 1′-hydroxymidazolam was compared with that observed before the administration of esmethadone (Fig. 1). The demographic characteristics of the healthy volunteers enrolled in the study are reported in Table S1 of the ESM.

As shown in Fig. 5, esmethadone did not significantly modify the C_{max} and AUC of midazolam (CYP3A4 substrate) [C_{max}: 11,500 ± 3350 pg/mL vs 9920 ± 2580 pg/mL; AUC: 25,500 ± 9210 h*pg/mL vs 24,500 ± 7350 h*pg/mL], while significant increases of C_{max} and AUC of 1′-hydroxymidazolam were observed (C_{max}: 5440 ± 3520 pg/mL vs 13,100 ± 4930 pg/mL; AUC: 10,700 ± 7360 h*pg/mL vs 41,100 ± 14,500 h*pg/mL of midazolam alone or co-administered with esmethadone). The pharmacokinetic parameters of midazolam and 1′-hydroxymidazolam in response to the co-administration with esmethadone are reported in Table 10.

Taken together, these data indicate a negligible effect of esmethadone on CYP3A4 activity. Coherently, the half-life

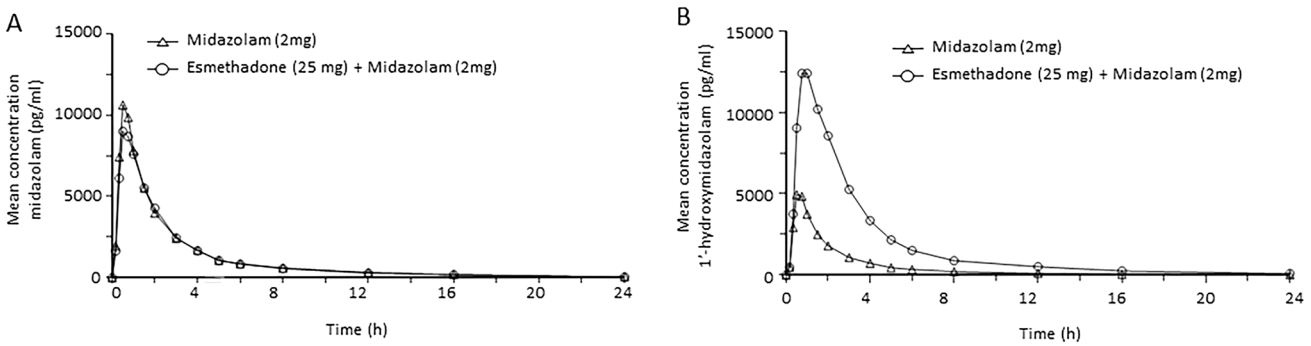

Fig. 5 Plasma time profile concentrations of midazolam (**A**) and 1′-hydroxymidazolam (**B**) after administration of midazolam alone (2 mg) or in combination with esmethadone (25 mg). *h* hours

Table 10 Effect of esmethadone (25 mg) on the pharmacokinetic parameters of CYP3A4 substrate midazolam and its metabolite 1′-hydroxymidazolam

Pharmacokinetic parameters	Midazolam alone Analyte: midazolam	Midazolam + esmethadone	Midazolam alone Analyte: 1′-hydroxymidazolam	Midazolam + esmethadone
C_{max} (pg/mL)	11,500 ± 3350	9920 ± 2580	5440 ± 3520	13,100 ± 4930
T_{max} (h)[a]	0.500 (0.333–1.08)	0.500 (0.333–1.00)	0.500 (0.500–0.750)	0.925 (0.500–2.00)*
AUC_{0-t} (h*pg/mL)	25,500 ± 9210	24,500 ± 7350	10,700 ± 7360	41,100 ± 14,500
AUC_{0-inf} (h*pg/mL)	26,800 ± 9740	25,900 ± 7730	11,600 ± 8260	42,700 ± 15100
$T_{1/2, el}$ (h)	5.12 ± 1.92	5.34 ± 1.80	3.68 ± 2.25	4.82 ± 1.59
CL/F (L/h)	83.8 ± 27.9	84.5 ± 27.5		
V_d/F (L)	571 ± 182	608 ± 160		

Data are expressed as arithmetic mean ± standard deviation

AUC_{0-t} area under the concentration–time curve from time zero to the time of the last quantifiable concentration, *AUC_{0-inf}* area under the concentration–time curve from time zero extrapolated to infinity, *CL/F* apparent clearance, *C_{max}* maximum observed concentration, *CYP* cytochrome P450, *T_{max}* time to C_{max}, *V_d/F* apparent volume of distribution, *$p < 0.001$ vs midazolam alone by Wilcoxon signed-rank test

[a] T_{max} is presented as median (range)

time of midazolam (5.12 ± 1.92 h) and 1′-hydroxymidazolam (3.68 ± 2.25 h) were not altered by esmethadone (5.34 ± 1.80 h vs 4.82 ± 1.59 h for midazolam and 1′-hydroxymidazolam, respectively). These data suggest that esmethadone does not affect the metabolism and elimination of 1′-hydroxymidazolam but rather its bioavailability and/or gastrointestinal absorption.

The investigation on the CYP2D6 activity led to the observation that esmethadone (loading dose of 75 mg) significantly increased the exposure of both dextromethorphan (CYP2D6 probe substrate) and its metabolite dextrorphan (Fig. 6). In particular, the AUC of dextromethorphan raised from 31,200 ± 80,800 h*pg/mL to 84,600 ± 130,000 h*pg/mL (2.71-fold increase). A similar effect was observed with dextromethorphan metabolite dextrorphan (27,200 ± 12,300 h*pg/mL vs 84,700 ± 30,400 *pg/mL; 3.11-fold increase). The pharmacokinetic parameters of dextromethorphan and dextrorphan in response to the co-administration with esmethadone are reported in Table 11.

Thus, the results of this study demonstrated that esmethadone is a moderate inhibitor of CYP2D6. Importantly, from the safety point of view, esmethadone was well tolerated in healthy participants when administered alone or in combination with dextromethorphan and midazolam (Table S2 of the ESM).

3.2.3 Study 3

The in vitro analysis with recombinant CYP450 enzymes demonstrated that esmethadone is mainly metabolized by CYP2B6 and CYP3A4 (Fig. 3). Thus, inhibition of CYP3A4 may have a clinically relevant impact on the pharmacokinetics and exposure of esmethadone. To test this hypothesis, we conducted a clinical study aimed at evaluating the effect of CYP34A inhibitor cobicistat on the esmethadone pharmacokinetic profile. The demographic characteristics of the healthy volunteers enrolled in the study are reported in Table S3 of the ESM.

Plasma concentration–time profiles after administration of esmethadone alone and in combination with cobicistat are presented in Fig. 7. Mean peak concentrations of esmethadone after co-administration with cobicistat on

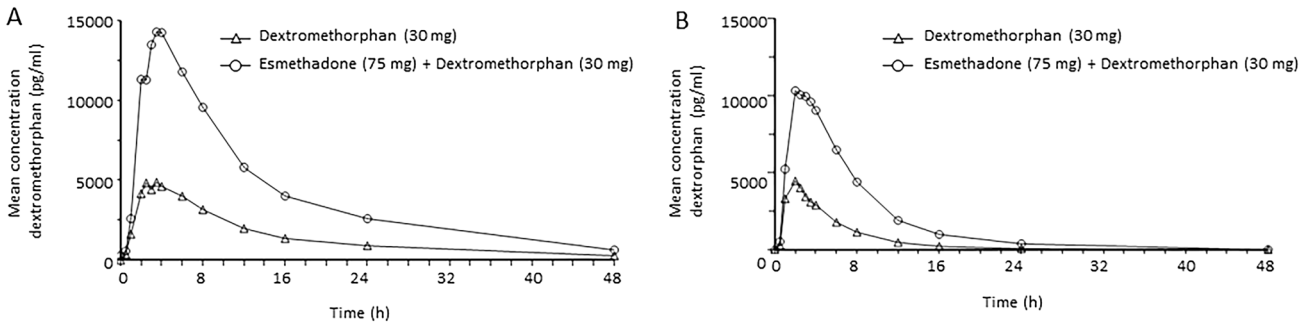

Fig. 6 Pharmacokinetic profile of dextromethorphan (**A**) and dextrorphan (**B**) after administration of dextromethorphan alone or in combination with esmethadone (75 mg). *h* hours

Table 11 Effect of esmethadone (75 mg) on the pharmacokinetic parameters of CYP2D6 substrate dextromethorphan and its substrate dextrorphan

Pharmacokinetic parameters	Dextromethorphan alone	Dextromethorphan + esmethadone	Dextromethorphan alone	Dextromethorphan + esmethadone
	Analyte: dextromethorphan		Analyte: dextrorphan	
C_{max} (pg/mL)	2200 ± 3800	6280 ± 5970	4900 ± 2620	11,500 ± 4790
T_{max} (h)[a]	2.50 (1.00–4.00)	3.00 (2.00–6.00)*	2.00 (1.00–3.50)	2.50 (1.00–4.15)*
AUC_{0-t} (h*pg/mL)	26,600 ± 66,100	77,200 ± 109,000	26,300 ± 12,100	82,900 ± 30,600
AUC_{0-inf} (h*pg/mL)	31,200 ± 80,800	84,600 ± 130,000	27,200 ± 12,300	84,700 ± 30,400
$T_{1/2, el}$ (h)	7.15 ± 3.29	8.90 ± 2.87	5.64 ± 4.97	5.80 ± 2.86
CL/F (L/h)	4560 ± 3280	907 ± 715		
V_d/F (L)	39,000 ± 24,800	10,700 ± 8470		

Data are expressed as arithmetic mean ± standard deviation

AUC_{0-t} area under the concentration–time curve from time zero to the time of the last quantifiable concentration, *AUC_{0-inf}* area under the concentration–time curve from time zero extrapolated to infinity, *CL/F* apparent clearance, *C_{max}* maximum observed concentration, *T_{max}* time to C_{max}, *V_d/F* apparent volume of distribution, *$p < 0.001$ vs dextromethorphan alone by Wilcoxon signed-rank test

[a]T_{max} is presented as median (range)

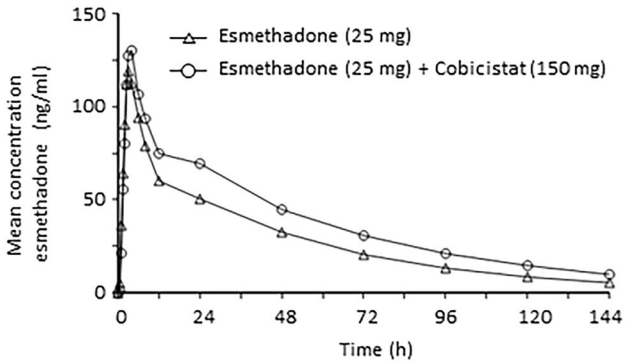

Fig. 7 Pharmacokinetic profile of esmethadone alone (25 mg) and after administration of cytochrome P450 3A4 inhibitor cobicistat (150 mg). *h* hours

Table 12 Effect of CYP3A4 inhibitor cobicistat (150 mg) on esmethadone (25 mg) pharmacokinetic parameters

Pharmacokinetic parameters	Esmethadone	Esmethadone + cobicistat
C_{max} (ng/mL)	131 ± 31.5	138 ± 25.5
T_{max}[a] (h)	2.50 (1.49–6.00)	3.02 (2.52–4.07)
AUC_{0-t} (h*ng/mL)	4100 ± 1210	5560 ± 1450
AUC_{0-inf} (h*ng/mL)	4430 ± 1370	6260 ± 1920
$T_{1/2,el}$ (h)	36.3 ± 7.36	43.4 ± 10.3
CL/F (L/h)	6.25 ± 2.21	4.37 ± 1.43
V_d/F (L)	310 ± 61.3	259 ± 45.9

Data are expressed as arithmetic mean ± standard deviation

AUC_{0-t} area under the concentration–time curve from time zero to the time of the last quantifiable concentration, *AUC_{0-inf}* area under the concentration–time curve from time zero extrapolated to infinity, *CL/F* apparent clearance, *C_{max}* maximum observed concentration, *CYP* cytochrome P450, *T_{max}* time to C_{max}, *V_d/F* apparent volume of distribution

[a]T_{max} is presented as median (range)

day 15 were similar to those measured after the administration of esmethadone alone (day 1). Maximum observed concentration of esmethadone was 119 ± 34.3 ng/mL when administered alone and 130 ± 22.5 ng/mL when co-administered with cobicistat. There was no apparent difference in the T_{max} of esmethadone (3.00 vs 4.00 h post-dose) or the shape of the concentration–time profiles.

Co-administration of esmethadone with cobicistat had only a slight impact on esmethadone pharmacokinetics. Mean esmethadone C_{max}, AUC_{0-t}, and AUC_{0-inf} values were comparable between treatments (Table 12). Median esmethadone T_{max} was similar when administered alone or co-administered with cobicistat (2.50 h vs 3.02 h). Mean esmethadone half-life, apparent clearance, and apparent volume of distribution values were also similar for both treatments (Table 12). No deaths, other serious adverse events, or other clinically significant adverse events occurred during the conduct of this study (Table S4 of the ESM).

Thus, the co-administration of repeated once-daily doses of the strong CYP3A4 inhibitor cobicistat did not impact the peak exposure (C_{max}) of esmethadone but did appear to have a slight effect on the total exposure (AUCs) of the drug. In the presence of cobicistat, the geometric mean ratios for esmethadone C_{max}, AUC_{0-t}, and AUC_{0-inf} were 105%, 134%, and 132%, respectively.

4 Discussion

The present studies were conducted to characterize potentially relevant metabolic pathways of esmethadone. The in vitro analysis indicated that esmethadone is mainly metabolized by CYP2B6 and CYP3A4. As previously described in patients [29], EDDP accounted for > 90% of in vitro metabolites. In vitro results also showed a potentially relevant inhibitory action of esmethadone on CYP2D6 and an inducing activity of CYP3A4. The IC_{50} value of CYP2D6 inhibition (9.6 µM) is indeed not far from the maximal exposure of esmethadone (C_{max}) observed in a phase I clinical trial (up to 3.2 µM) [7]. The K_i for CYP2D6 by unbound esmethadone was determined to be 1.74 µM. This value can be utilized to predict a possible DDI in vivo by using equations and cut-off values recommended in the FDA DDI guidance: R1 = $1 + (I_{max,u}/K_{i,u})$, where $I_{max,u}$ (or $C_{max,u}$) is the maximal unbound esmethadone concentration in plasma at steady state. The $C_{max,u}$ is 0.587 µM, as previously determined [7]. The cut-off value for R1 is equal to 1.02. Thus, for CYP2D6, the R1 equation with the experimentally determined values inserted is: $C_{max,u}/K_{i,u} = 1 + (0.587\ \mu M/1.74\ \mu M) = 1.33$. This value is greater than the cut-off value (1.02), indicating clinical DDI studies are needed to better understand potential clinical implications. Thus, to test the possibility that esmethadone may have an impact on drugs metabolized by CYP2D6 (inhibition) and CYP3A4 (induction), we conducted a clinical trial to assess the effect of a single loading dose of esmethadone on the pharmacokinetics of dextromethorphan (CYP2D6 probe substrate) and the effect of repeated doses of esmethadone on the pharmacokinetics of midazolam (CYP3A4 probe substrate) in healthy participants.

Esmethadone did not significantly modify the C_{max} and AUC of midazolam, while it significantly increased the C_{max} and AUC of 1′-hydroxymidazolam. Thus, in accordance with current FDA guidelines, it can be suggested that esmethadone does not induce CYP3A4 enzyme activity. However, the analysis of the metabolite 1′-hydroxymidazolam demonstrated a significant increase of AUC (3.84-fold). The enzymatic metabolism of midazolam involves the CYP3A4 pathway, generating 1′-hydroxymidazolam, which then undergoes phase II metabolism by glucuronidation [30]. Importantly, the half-life time of 1′-hydroxymidazolam is similar to that of the parent drug, 1.72 h [30]. Thus, the decline of metabolite in plasma is controlled also by elimination of the parent drug. Concentration of 1′-hydroxymidazolam declines in parallel with midazolam [31]. In our study, we observed a very similar half-life time of midazolam (5.12 ± 1.92 h) and 1′-hydroxymidazolam (3.68 ± 2.25 h) and these values were not meaningfully altered by esmethadone (5.34 ± 1.80 h vs 4.82 ± 1.59 h for midazolam and 1′-hydroxymidazolam, respectively). These data suggest that esmethadone does not affect the metabolism and elimination of 1′-hydroxymidazolam but may instead affect its bioavailability or gastrointestinal production.

The impact of generation of 1′-hydroxymidazolam from midazolam during the first pass can be seen in the three-times higher value of the 1′-hydroxymidazolam-to-midazolam AUC ratio after the drug oral dose compared with the value obtained after the intravenous dose [30]. As the intrinsic activities of gut and liver CYP3A have been observed to be similar [32, 33], fractions of midazolam converted to two primary CYP3A metabolites in the intestine are assumed to be identical in the liver [34]. On the contrary, conjugation is considered significantly lower in the intestine owing to the relative low expression of UGT enzymes. Thus, it is conceivable to hypothesize that esmethadone induced the generation of 1′-hydroxymidazolam from midazolam at the gastrointestinal level, as previously hypothesized with methadone itself [12, 35], although the metabolism and clearance of midazolam metabolites are governed by a complex interplay of multiple factors. Thus, the clinical impact of esmethadone on the pharmacokinetics of drugs metabolized by CYP3A4 may be multi-faceted.

Predicting if the 3.84-fold increase of 1′-hydroxymidazolam by esmethadone may have a clinical impact is difficult. However, in our study, we did not find any increase of adverse effects when the two drugs were co-administered, although the period of treatment was short. Considering the increased of exposure of this metabolite, it is important to take into consideration that the AUC of 1′-hydroxymidazolam is approximately one third of that of midazolam, and thus it is considered to only partially account for the pharmacological effect. In the presence of esmethadone, the exposure of midazolam plus its metabolite increased by 1.78-fold, an effect that is more likely to be considered not clinically relevant.

Results from the in vitro analysis indicated that esmethadone may have a significant inhibitory activity on CYP2D6. Indeed, esmethadone significantly increased the AUC of dextromethorphan (CYP2D6 probe substrate) and its metabolite by 2.71-fold and 3.11-fold, respectively. Thus, in accordance with current FDA guidelines, esmethadone can be considered a moderate CYP2D6 inhibitor. Importantly, from the safety point of view, esmethadone was well tolerated in healthy subjects when administered alone or in combination with dextromethorphan and midazolam. In contrast, methadone is not metabolized by CYP2D6; indeed, fluoxetine and paroxetine, potent CYP2D6 inhibitors [36] and drugs widely employed in the treatment of depression, do not change the metabolism of methadone [37].

The increased exposure of dextrorphan after esmethadone administration is in contrast with the effects observed with the other CYP2D6 inhibitor quinidine, which greatly increases the amount of circulating dextromethorphan and decreases the metabolite dextrorphan [38]. The reasons underlying this opposite effect on metabolite exposure by two CYP2D6 inhibitors are unclear and suggest different effects of these two drugs on other metabolic pathways. It should be noticed that quinidine, in addition to inhibiting CYP2D6, displays different effects on CYP3A4 metabolic activities, dependent on the substrate used, which range from strong inhibition to even activation [39]. In contrast, dextrorphan is further metabolized by CYP3A4 and UGT enzymes [38]. Although the esmethadone UGT inhibitory activity is too limited to be considered significant, this observation may at least in part explain the observed increase of dextrorphan disposition.

We also evaluated the influence of CYP3A4 inhibition on esmethadone metabolism. Because of the paradoxical results obtained with the potent CYP3A4 inhibitors ritonavir [22], nelfinavir [25], indinavir [40] ritonavir/indinavir [26], and atazanavir [27], we decided to utilize cobicistat. This CYP3A4 inhibitor increased the C_{max}, AUC_{0-t}, and AUC_{0-inf} of esmethadone by 105%, 134%, and 132%, respectively. These data indicate that esmethadone is partially metabolized by CYP3A4 but exclude a significant interaction with strong CYP3A4 inhibitors and inducers. Indeed, CYP inhibition studies support a more predominant role for CYP2B6 than for CYP3A4 in determining methadone disposition, as changes in plasma R/S methadone ratios observed after rifampin (CYP2B6 and CYP3A4 inducer) or troleandomycin (CYP3A4 inhibitor) pre-treatment in humans were successfully predicted by CYP2B6-catalyzed but not CYP3A4-catalyzed methadone N-demethylation [41]. In addition, no correlation between methadone clearance (intravenous and oral) and CYP3A4/5 activity (hepatic and intestinal) has been observed [24], data that further support a meaningful role for CYP3A4/5 in clinical methadone N-demethylation and clearance, in contrast with in vitro results. Thus, in vivo, CYP2B6 appears to be the major determinant of methadone metabolism and disposition, and CYP2B6 activity and stereoselective metabolic interactions may confer variability in methadone disposition [41]. This assumption has also been demonstrated by the fact that the R/S methadone ratio is stable in patients co-treated with the CYP2B6 inhibitor ticlopidine, compared with control untreated subjects [42]. The involvement of CYP2B6 on methadone metabolism has also been confirmed by genetic studies conducted on subjects carrying different single nucleotide polymorphisms of this gene [43–45]. In addition, our in vitro data indicating a significant induction of CYP2B6 by esmethadone, may contribute, together with CYP3A4, to the slight but significant decrease in its bioavailability observed after repeated doses of drug administration [12]. Thus, esmethadone is primarily metabolized by CYP2B6 not only in vitro but also in vivo.

Finally, the clearance of esmethadone is well balanced between the kidney and liver, thus suggesting minimal accumulation in patients with impaired organ functions. This hypothesis may need confirmation with adequate clinical studies.

The possible clinical implication of inhibitory action of esmethadone on drug transporter OCT1 and P-gp needs further investigations. Indeed, OCT1 is mainly expressed in the liver where it can mediate the uptake of many drugs, including metformin, imatinib, anthracyclines, oxaliplatin, and sorafenib [46]. Even more relevant could be the inhibition of P-gp that may increase the gastrointestinal absorption, and thus the bioavailability, of many drugs including the direct oral anticoagulants (apixaban, edoxaban, rivaroxaban and dabigatran) [47], and many others. In addition, a single nucleotide polymorphism of P-gp has been associated with a 32.9% higher concentration of methadone [48], thus suggesting that esmethadone is also a substrate of this drug efflux transporter that may influence its disposition in some patients.

5 Conclusions

These studies indicate that the administration of esmethadone increases the exposure of drugs metabolized by CYP2D6. No significant interaction is predicted with CYP3A4 inhibitors and with CYP3A4 metabolized drugs, confirming previous in vitro and in vivo evidence, indicating that the metabolism of esmethadone is more related to CYP2B6 than to CYP3A activity.

Supplementary Information The online version contains supplementary material available at https://doi.org/10.1007/s40268-023-00450-6.

Declarations

Funding This research was sponsored by Relmada Therapeutics, Inc., Coral Gables, FL, USA.

Conflict of interest Sara De Martin received personal fees from Relmada Therapeutics and from Aesculapius Farmaceutici. Marco Pappagallo received personal fees from Relmada Therapeutics during this study, he holds stock ownership with Acadia, and he has received personal fees from Overlook Medical Center. Andrea Mattarei and Franco Folli received personal fees from Relmada Therapeutics. Sergio Traversa, Charles E. Inturrisi, and Paolo L. Manfredi received personal fees and or held stock ownership from Relmada Therapeutics. Sergio Traversa is an employee of Relmada Therapeutics. Paolo L. Manfredi and Charles E. Inturrisi are inventors on patents related to esmethadone. Clotilde Guidetti has received personal fees from MGGM Therapeutics. James Stuart received fees from Relmada as a paid consultant.

Ethics approval Not applicable.

Consent to participate Not applicable.

Consent for publication Not applicable.

Availability of data and material The datasets generated and/or analyzed during the current study are available from the corresponding author on reasonable request.

Code availability Not applicable.

References

1. Low Y, Setia S, Lima G. Drug-drug interactions involving antidepressants: focus on desvenlafaxine. Neuropsychiatr Dis Treat. 2018;14:567–80.
2. Henningfield J, Gauvin D, Bifari F, Fant R, Shram M, Buchhalter A, et al. REL-1017 (esmethadone; D-methadone) does not cause reinforcing effect, physical dependence and withdrawal signs in Sprague Dawley rats. Sci Rep. 2022;12(1):11389.
3. Shram M, Henningfield J, Apseloff G, Gorodetzky C, De Martin S, Vocci F, et al. No meaningful abuse potential in recreational ketamine users of REL-1017 (esmethadone hydrochloride), a new NMDAR antagonist and potential rapid-acting antidepressant. Presented at: American Society of Clinical Psychopharmacology (ASCP) Annual Meeting; Scottsdale (AZ); 31, 2022.
4. Bettini E, De Martin S, Mattarei A, Pappagallo M, Stahl SM, Bifari F, et al. The *N*-methyl-D-aspartate receptor blocker REL-1017 (esmethadone) reduces calcium influx induced by glutamate, quinolinic acid, and gentamicin. Pharmaceuticals (Basel). 2022;15(7):882.
5. Bettini E, Stahl SM, De Martin S, Mattarei A, Sgrignani J, Carignani C, et al. Pharmacological comparative characterization of REL-1017 (esmethadone-HCl) and other NMDAR channel blockers in human heterodimeric *N*-methyl-D-aspartate receptors. Pharmaceuticals (Basel). 2022;15(8):997.
6. Fava M, Stahl S, Pani L, De Martin S, Pappagallo M, Guidetti C, et al. REL-1017 (esmethadone) as adjunctive treatment in patients with major depressive disorder: a phase 2a randomized double-blind trial. Am J Psychiatry. 2022;179(2):122–31.
7. Bernstein G, Davis K, Mills C, Wang L, McDonnell M, Oldenhof J, et al. Characterization of the safety and pharmacokinetic profile of D-methadone, a novel *N*-methyl-D-aspartate receptor antagonist in healthy, opioid-naive subjects: results of two phase 1 studies. J Clin Psychopharmacol. 2019;39(3):226–37.
8. Meresaar U, Nilsson MI, Holmstrand J, Anggard E. Single dose pharmacokinetics and bioavailability of methadone in man studied with a stable isotope method. Eur J Clin Pharmacol. 1981;20(6):473–8.
9. Wolff K, Hay AW, Raistrick D, Calvert R. Steady-state pharmacokinetics of methadone in opioid addicts. Eur J Clin Pharmacol. 1993;44(2):189–94.
10. Wolff K, Rostami-Hodjegan A, Shires S, Hay AW, Feely M, Calvert R, et al. The pharmacokinetics of methadone in healthy subjects and opiate users. Br J Clin Pharmacol. 1997;44(4):325–34.
11. Kristensen K, Blemmer T, Angelo HR, Christrup LL, Drenck NE, Rasmussen SN, et al. Stereoselective pharmacokinetics of methadone in chronic pain patients. Ther Drug Monit. 1996;18(3):221–7.
12. Nilsson MI, Anggard E, Holmstrand J, Gunne LM. Pharmacokinetics of methadone during maintenance treatment: adaptive changes during the induction phase. Eur J Clin Pharmacol. 1982;22(4):343–9.
13. Gourlay GK, Cherry DA, Cousins MJ. A comparative study of the efficacy and pharmacokinetics of oral methadone and morphine in the treatment of severe pain in patients with cancer. Pain. 1986;25(3):297–312.
14. Garrido MJ, Troconiz IF. Methadone: a review of its pharmacokinetic/pharmacodynamic properties. J Pharmacol Toxicol Methods. 1999;42(2):61–6.
15. Ketter TA, Flockhart DA, Post RM, Denicoff K, Pazzaglia PJ, Marangell LB, et al. The emerging role of cytochrome P450 3A in psychopharmacology. J Clin Psychopharmacol. 1995;15(6):387–98.
16. Moody NB, Smith PL. Proactive changes in nursing work force development in Tennessee. J Nurs Adm. 1997;27(12):4–7.
17. Gerber JG, Rhodes RJ, Gal J. Stereoselective metabolism of methadone N-demethylation by cytochrome P4502B6 and 2C19. Chirality. 2004;16(1):36–44.
18. Iribarne C, Berthou F, Baird S, Dreano Y, Picart D, Bail JP, et al. Involvement of cytochrome P450 3A4 enzyme in the N-demethylation of methadone in human liver microsomes. Chem Res Toxicol. 1996;9(2):365–73.
19. Foster DJ, Somogyi AA, Bochner F. Methadone N-demethylation in human liver microsomes: lack of stereoselectivity and involvement of CYP3A4. Br J Clin Pharmacol. 1999;47(4):403–12.
20. Wang JS, DeVane CL. Involvement of CYP3A4, CYP2C8, and CYP2D6 in the metabolism of (R)- and (S)-methadone in vitro. Drug Metab Dispos. 2003;31(6):742–7.
21. Kharasch ED, Hoffer C, Whittington D, Sheffels P. Role of hepatic and intestinal cytochrome P450 3A and 2B6 in the metabolism, disposition, and miotic effects of methadone. Clin Pharmacol Ther. 2004;76(3):250–69.
22. Bruce RD, Altice FL, Gourevitch MN, Friedland GH. Pharmacokinetic drug interactions between opioid agonist therapy and antiretroviral medications: implications and management for clinical practice. J Acquir Immune Defic Syndr. 2006;41(5):563–72.
23. Gerber JG, Rosenkranz S, Segal Y, Aberg J, D'Amico R, Mildvan D, et al. Effect of ritonavir/saquinavir on stereoselective pharmacokinetics of methadone: results of AIDS Clinical Trials Group (ACTG) 401. A cquir Immune Defic Syndr. 2001;27(2):153–60.
24. Kharasch ED, Bedynek PS, Park S, Whittington D, Walker A, Hoffer C. Mechanism of ritonavir changes in methadone pharmacokinetics and pharmacodynamics: I. Evidence against CYP3A mediation of methadone clearance. Clin Pharmacol Ther. 2008;84(4):497–505.
25. Kharasch ED, Walker A, Whittington D, Hoffer C, Bedynek PS. Methadone metabolism and clearance are induced by nelfinavir despite inhibition of cytochrome P4503A (CYP3A) activity. Drug Alcohol Depend. 2009;101(3):158–68.
26. Kharasch ED, Hoffer C, Whittington D, Walker A, Bedynek PS. Methadone pharmacokinetics are independent of cytochrome P4503A (CYP3A) activity and gastrointestinal drug transport: insights from methadone interactions with ritonavir/indinavir. Anesthesiology. 2009;110(3):660–72.

27. Friedland G, Andrews L, Schreibman T, Agarwala S, Daley L, Child M, et al. Lack of an effect of atazanavir on steady-state pharmacokinetics of methadone in patients chronically treated for opiate addiction. AIDS. 2005;19(15):1635–41.
28. US Department of Health and Human Services, Food and Drug Administration, Center for Drug Evaluation and Research (CDER). Guidance for industry: clinical drug interaction studies: cytochrome P450 enzyme- and transporter-mediated drug interactions. 2020. https://www.fda.gov/media/134581/download. Accessed 13 Nov 2023.
29. Foster DJ, Somogyi AA, Dyer KR, White JM, Bochner F. Steady-state pharmacokinetics of (R)- and (S)-methadone in methadone maintenance patients. Br J Clin Pharmacol. 2000;50(5):427–40.
30. Nguyen HQ, Kimoto E, Callegari E, Obach RS. Mechanistic modeling to predict midazolam metabolite exposure from in vitro data. Drug Metab Dispos. 2016;44(5):781–91.
31. Mandema JW, Tuk B, van Steveninck AL, Breimer DD, Cohen AF, Danhof M. Pharmacokinetic-pharmacodynamic modeling of the central nervous system effects of midazolam and its main metabolite alpha-hydroxymidazolam in healthy volunteers. Clin Pharmacol Ther. 1992;51(6):715–28.
32. Gertz M, Harrison A, Houston JB, Galetin A. Prediction of human intestinal first-pass metabolism of 25 CYP3A substrates from in vitro clearance and permeability data. Drug Metab Dispos. 2010;38(7):1147–58.
33. von Richter O, Burk O, Fromm MF, Thon KP, Eichelbaum M, Kivisto KT. Cytochrome P450 3A4 and P-glycoprotein expression in human small intestinal enterocytes and hepatocytes: a comparative analysis in paired tissue specimens. Clin Pharmacol Ther. 2004;75(3):172–83.
34. Paine MF, Khalighi M, Fisher JM, Shen DD, Kunze KL, Marsh CL, et al. Characterization of interintestinal and intraintestinal variations in human CYP3A-dependent metabolism. J Pharmacol Exp Ther. 1997;283(3):1552–62.
35. Oda Y, Kharasch ED. Metabolism of methadone and levo-alpha-acetylmethadol (LAAM) by human intestinal cytochrome P450 3A4 (CYP3A4): potential contribution of intestinal metabolism to presystemic clearance and bioactivation. J Pharmacol Exp Ther. 2001;298(3):1021–32.
36. Alfaro CL, Lam YW, Simpson J, Ereshefsky L. CYP2D6 inhibition by fluoxetine, paroxetine, sertraline, and venlafaxine in a crossover study: intraindividual variability and plasma concentration correlations. J Clin Pharmacol. 2000;40(1):58–66.
37. Victorri-Vigneau C, Verstuyft C, Bouquie R, Laforgue EJ, Hardouin JB, Leboucher J, et al. Relevance of CYP2B6 and CYP2D6 genotypes to methadone pharmacokinetics and response in the OPAL study. Br J Clin Pharmacol. 2019;85(7):1538–43.
38. Taylor CP, Traynelis SF, Siffert J, Pope LE, Matsumoto RR. Pharmacology of dextromethorphan: relevance to dextromethorphan/quinidine (Nuedexta®) clinical use. Pharmacol Ther. 2016;164:170–82.
39. Galetin A, Clarke SE, Houston JB. Quinidine and haloperidol as modifiers of CYP3A4 activity: multisite kinetic model approach. Drug Metab Dispos. 2002;30(12):1512–22.
40. Kharasch ED, Bedynek PS, Hoffer C, Walker A, Whittington D. Lack of indinavir effects on methadone disposition despite inhibition of hepatic and intestinal cytochrome P4503A (CYP3A). Anesthesiology. 2012;116(2):432–47.
41. Totah RA, Allen KE, Sheffels P, Whittington D, Kharasch ED. Enantiomeric metabolic interactions and stereoselective human methadone metabolism. J Pharmacol Exp Ther. 2007;321(1):389–99.
42. Kharasch ED, Stubbert K. Role of cytochrome P4502B6 in methadone metabolism and clearance. J Clin Pharmacol. 2013;53(3):305–13.
43. Wang SC, Ho IK, Tsou HH, Tian JN, Hsiao CF, Chen CH, et al. CYP2B6 polymorphisms influence the plasma concentration and clearance of the methadone S-enantiomer. J Clin Psychopharmacol. 2011;31(4):463–9.
44. Gadel S, Friedel C, Kharasch ED. Differences in methadone metabolism by CYP2B6 variants. Drug Metab Dispos. 2015;43(7):994–1001.
45. Kharasch ED, Regina KJ, Blood J, Friedel C. Methadone pharmacogenetics: CYP2B6 polymorphisms determine plasma concentrations, clearance, and metabolism. Anesthesiology. 2015;123(5):1142–53.
46. Brosseau N, Ramotar D. The human organic cation transporter OCT1 and its role as a target for drug responses. Drug Metab Rev. 2019;51(4):389–407.
47. Ferri N, Colombo E, Tenconi M, Baldessin L, Corsini A. Drug–drug interactions of direct oral anticoagulants (DOACs): from pharmacological to clinical practice. Pharmaceutics. 2022;14(6):1120.
48. Zahari Z, Lee CS, Ibrahim MA, Musa N, Mohd Yasin MA, Lee YY, et al. Relationship between ABCB1 polymorphisms and serum methadone concentration in patients undergoing methadone maintenance therapy (MMT). Am J Drug Alcohol Abuse. 2016;42(5):587–96.